Int. J. Heat Mass Transfer. Vol. 28, No. 1, pp. 81–90, 1985
Printed in Great Britain

0017–9310/85 $3.00 + 0.00

Downward heat transfer in heat-generating boiling pools*

T. C. CHAWLA and J. D. BINGLE
Reactor Analysis and Safety Division, Argonne National Laboratory, Argonne, IL 60439, U.S.A.

(*Received* 23 *December* 1983 *and in revised form* 30 *April* 1984)

Abstract—A model for heat transfer from the horizontal base of a volume heated boiling pool is proposed. Because of the density difference caused by volume boiling between the bulk fluid and the fluid near the base, the lighter two-phase fluid causes movement of the bulk fluid in the upward direction and causes a negative pressure gradient along the base plate of the pool. This negative pressure drives returning subcooled single-phase liquid in the boundary layer along the base plate. The analysis for the laminar case provides the definition of equivalent Grashof number for the combined (or opposing) two-phase and temperature driven natural convection along the base plate. The turbulent boundary layer is analyzed by assuming a two-layer model in which the inner layer is characterized by viscous and conduction terms and the outer layer by mean convection terms. The similarity analysis of the governing equations yields universal profiles for temperature and velocity and the scaling laws for the inner and outer layers. An asymptotic matching of the temperature profile in the overlap region leads to a heat transfer law that correlates the available experimental data on a volume heated boiling pool satisfactorily.

INTRODUCTION

THE PHENOMENON of heat transfer from volumetric heated boiling pools in the downward direction is of considerable interest in nuclear reactor safety analysis. For example, in the post-accident heat removal (PAHR) studies of liquid metal cooled fast breeder reactors (LMFBRs), it is of interest to determine heat transfer to the boiling stainless steel liquid film in molten pool penetration of an MgO substrate. The bubbles rising from the boiling of a stainless steel film lying at the bottom of a heat generating pool consisting of a MgO and UO_2 eutectic solution, causes the upward motion of the bulk fluid. The buoyancy effect of the two-phase bulk fluid generates a negative pressure gradient along the base resulting in motion of the single-phase fluid in the boundary layer over the stainless steel liquid film. Because of heat generation in the molten pool, the temperature of the pool is expected to be higher than the saturation temperature of stainless steel, hence the bubbles formed due to boiling of the stainless steel film do not condense in the bulk of the pool and continue to maintain convection currents until the whole thickness of the film is boiled off.

The heat transfer from concrete substrate during molten pool penetration or during sodium–concrete interaction also takes place due to convection driven by gas and water vapor bubbles released from the concrete substrate heatup and due to chemical reactions at the interface. Similarly downward heat transfer in the boiling pool of stainless steel and fuel mixture pertaining to the transition phase of hypothetical core disruptive accidents is of considerable interest in predicting the dynamics of the pool.

Besides the above-mentioned applications, the cooling of the modern electronic components characterized by relatively high heat fluxes, takes place through volume boiling which causes convection currents and subsequently rejection of heat to a horizontally submerged condenser [1]. The heat transfer from internally heated boiling pools is also of potential interest in chemical reactor engineering.

The initial preliminary experimental study of downward heat transfer from heat generating boiling pools was carried out by Stein *et al.* [2]. Subsequently their work was extended with various refinements by Gabor *et al.* [3]. Besides the measurements of the downward heat flux, these authors also performed visual studies of the flow pattern along the base of the pool. Since the base was cooler than the bulk of the fluid, the temperature gradient at the base opposed the natural convection motion driven by the buoyancy effect of the two-phase mixture in the bulk of the pool. Consequently, at low boiling rates, these authors observed a wave of cold liquid washing back and forth across the base, and at higher boiling rates the normal convection currents typical of boiling pools were established.

Subsequently, two other somewhat related studies were carried out by Paik *et al.* [4] and by Greene and Schwarz [5]. Paik *et al.* conducted a series of experiments to simulate the heat transfer characteristics of molten core debris pools growing in the concrete. The molten core debris–concrete system was simulated by using a volumetrically heated pool with gas injection at the pool boundaries. They correlated their data based on superficial gas velocity and characteristic bubble dimension. This method of correlation of their data is distinctly different from the method presented here. The characteristic velocity is

* This work was performed under the auspices of the U.S. Department of Energy.

NOMENCLATURE

A	integration constant in equation (55a)
A_k	coefficients of expansion for characteristic velocity in the laminar boundary layer
B	integration constant in equation (55b)
B_k	coefficients of expansion for boundary layer thickness for laminar flow
B_k^*	constants defined by equations (31)
C'	parameter defined by equation (56)
C	parameter defined in equation (59)
C_p	specific heat at constant pressure
F'	velocity profile for outer layer, $(u-U_m)/u_0$
f'	velocity profile for inner layer, u/U_I
G	nondimensional turbulent shear stress
Gr	Grashof number based on pool height L, $(\beta\Delta T_w+6\alpha)gL^3/\nu^2$
Gr_x	Grashof number based on characteristic length x
g	acceleration due to gravity
H	nondimensional total buoyancy function
h	heat transfer coefficient
K	thermal conductivity of liquid
L	pool height
m	exponent in expansion (27a) for characteristic velocity
n	exponent in expansion (27b) for boundary layer thickness
Nu_x	Nusselt number based on length x, hx/K
Nu	Nusselt number based on pool height L
P	pressure
P_h	hydrostatic pressure prevailing in two-phase medium outside the boundary layer
P_m	local dynamic pressure in the boundary layer
Pr	Prandtl number, $\mu C_p/K$
q_w	wall heat flux
$\dot{q}$	volumetric heat generation rate
Ra	Rayleigh number, $Pr\,Gr$
T	temperature
T'	turbulent fluctuations in temperature T
ΔT	$T-T_a$
ΔT_w	T_w-T_a
U	characteristic velocity in x-direction in the laminar boundary layer
U_0, U_1	first- and second-order nondimensional velocities in the expansion for U^*
U_m	velocity maximum
u	x-component of mean velocity in the boundary layer
u'	turbulent fluctuations in u-component
u_T	velocity scale for turbulent fluctuations in the outer layer
v	y-component of mean velocity in the boundary layer
v'	turbulent fluctuations in v-component
x	coordinate in direction parallel to the base as shown in Fig. 1
y	coordinate in direction normal to the wall.

Greek symbols

ξ	dimensionless inner variable, y/Λ
α	void fraction in the boiling pool
β	thermal expansion coefficient
δ	boundary layer thickness
δ_0, δ_1	first- and second-order nondimensional boundary layer thickness in the expansion for δ^*
ε	perturbation parameter defined by equations (21b) and (33)
ε_m	perturbation parameter defined by equation (33)
η	dimensionless outer variable, y/δ
θ	$(T-T_w)/\Delta T_I$
κ	universal constant in temperature profile (55)
λ	thermal diffusivity, $K/\rho C_p$
μ	dynamic viscosity
ν	kinematic viscosity
ρ	fluid density
Φ_I	scale for turbulent heat flux, $q_w/\rho_{la}C_p$
ϕ	nondimensional turbulent flux in the boundary layer
Ψ	$(T-T_\infty)/\Delta T_0$.

Subscripts

o	pertaining to the outer layer
a	pertaining to bulk fluid properties outside the boundary layer
I	pertaining to inner layer
g	pertaining to vapor phase
l	pertaining to liquid phase
s	pertaining to characteristic scale
w	pertaining to wall.

Superscripts

*	pertaining to nondimensional variables.

governed by natural convection driven by the buoyancy effect of two-phase flow. However, the characteristic velocity used by these authors is also expected to depend on the rate of injection of gas. Hence the rate of heat transfer may also be governed by forced flows governed by injection rates of the gas at the base of the pool.

Greene and Schwarz [5] studied heat transfer between overlying immiscible liquid layers with gas injection. They assumed two dominant modes of transfer. The first mode is driven by agitation at the interface caused by gas bubbling. The second mode is initiated at higher injection rates where the lower liquid layer is entrained in the form of droplets behind the rising bubbles as these burst through the interface. The entrained droplets transfer their sensible excess heat to the overlying liquid layer. However, these authors proposed a very preliminary correlation containing a number of adjustable parameters. The present study is not expected to simulate the second mode of heat transfer at the interface between overlying immiscible liquid layers. However, the first mode as identified by these authors should be simulated reasonably well by the turbulent natural convection (driven by the buoyancy effect of two-phase flow) model proposed here.

The present analytical study proposes a mechanism for downward heat transfer to the base of the pool and successfully attempts to correlate the heat transfer data of Gabor *et al.* [3]. The present analysis is a continuation of the principal author's work [6] on heat transfer from vertical/inclined boundaries of heat generating boiling pools.

GOVERNING EQUATIONS

The convection currents driven by the buoyancy effect of two-phase flow in the bulk of the pool cause fluid to be drawn along the base from either edges and then rise into the bulk fluid near the center of the base. For the unheated base plate, fluid near it is subcooled and therefore free from boiling. At large Rayleigh numbers (based on the height of the pool) the flow along the base can be assumed to be a single-phase boundary layer flow starting from the edges of the base plate. Outside the boundary the flow is assumed to be essentially stagnant consisting of a two-phase mixture. This model is depicted schematically in Fig. 1. Depending upon the values of Rayleigh numbers the flow may be laminar in the initial segment of the boundary layer and turbulent in the latter part. At very high Rayleigh numbers, the laminar part in the initial segment may not extend for more than a few millimeters and the turbulent part may almost extend over the whole segment. The analysis is carried out over a range of Rayleigh numbers high enough so that the boundary layer approximations are valid both in the laminar and turbulent segments. Consequently, the governing equations in the spirit of the Boussinesq approximation both for laminar and turbulent flows can be given as

$$\frac{\partial u}{\partial x}+\frac{\partial v}{\partial y}=0 \tag{1}$$

$$\rho\left(u\frac{\partial u}{\partial x}+v\frac{\partial u}{\partial y}\right)=-\frac{\partial P}{\partial x}+\mu\frac{\partial^2 u}{\partial y^2}+\frac{\partial}{\partial y}(-\overline{u'v'}) \tag{2}$$

$$-\frac{\partial P}{\partial y}+\rho g=0 \tag{3}$$

$$u\frac{\partial T}{\partial x}+v\frac{\partial T}{\partial y}=\lambda\frac{\partial^2 T}{\partial y^2}+\frac{\partial(-\overline{v'T'})}{\partial y}+\frac{\dot{q}}{\rho C_p} \tag{4}$$

where the symbols are defined in the nomenclature.

It is convenient to decompose the static pressure P into local hydrostatic pressure P_h prevailing in the two-phase medium outside the boundary layer, so that $\nabla P_h=-\rho_a \mathbf{g}$, and dynamic pressure P_m which arises due to motion. Consequently, we can write

$$\nabla P=\nabla P_m+\nabla P_h=\nabla P_m-\rho_a \mathbf{g}. \tag{5}$$

We may note that the Boussinesq approximation for natural convection flows consists of a two-part approximation: (a) it neglects all variable property effects in these governing equations except for the density variation in the momentum equation, and (b) it approximates this density through a simplified equation of state

$$\rho=\rho_{la}+\rho\beta(T-T_a). \tag{6}$$

Assuming further that the void fraction in the bulk of the pool is independent of height y from the bottom of the pool (see Fig. 1). In view of this assumption, the two-phase density ρ_a is given as

$$\rho_a=\alpha\rho_g+(1-\alpha)\rho_{la}. \tag{7}$$

Substituting equation (5) into equation (3) gives

$$-\frac{\partial P_m}{\partial y}+(\rho-\rho_a)g=0. \tag{8a}$$

The use of equations (6) and (7) gives

$$-\frac{\partial P_m}{\partial y}+[\alpha(\rho_{la}-\rho_g)+\rho\beta(T-T_a)]g=0 \tag{8b}$$

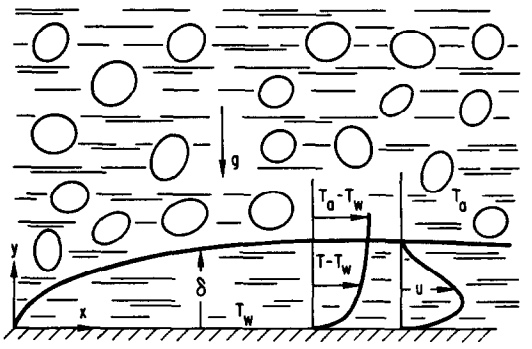

FIG. 1. Mechanistic model of downward heat transfer from volume heated boiling pool.

or

$$\frac{\partial P_m}{\partial y} = \rho_{la}[\alpha+\beta(T-T_a)]g \tag{8c}$$

where we assumed that $\rho_{la} \gg \rho_g$ and that $\rho \simeq \rho_{la}$, the latter approximation is consistent with Boussinesq's approximation. The use of equation (5) and the approximation $\rho \simeq \rho_{la}$ in equation (2) gives

$$u\frac{\partial u}{\partial x}+v\frac{\partial u}{\partial y} = -\frac{1}{\rho_{la}}\frac{\partial P_m}{\partial x}+\nu\frac{\partial^2 u}{\partial y^2}+\frac{1}{\rho_{la}}\frac{\partial}{\partial y}(-\overline{u'v'}). \tag{9}$$

The boundary conditions on equations (1), (9), (8), and (4) are

$$u, v = 0, T = T_w \quad \text{at} \quad y = 0 \tag{10a}$$

$$u, v = 0, P_m = 0, T = T_a \quad \text{at} \quad y = \delta. \tag{10b}$$

In writing down equation (10b), we have assumed that the momentum and thermal boundary layers are of equal thickness. This assumption is valid for moderate Prandtl number fluids of interest to the present study.

INTEGRAL METHOD OF ANALYSIS FOR LAMINAR FLOW

For laminar flow in the boundary layer, we drop the turbulent diffusion terms in equations (9) and (4) and integrate these equations together with equations (1) and (10), over the boundary layer thickness to obtain

$$\frac{\partial}{\partial x}\int_0^\delta u^2\,dy = -\frac{1}{\rho_{la}}\int_0^\delta \frac{\partial P_m}{\partial x}\,dy - \nu\left(\frac{\partial u}{\partial y}\right)_{y=0} \tag{11}$$

$$\frac{\partial}{\partial x}\int_0^\delta u(T-T_a)\,dy = -\lambda\left[\frac{\partial(T-T_a)}{\partial y}\right]_{y=0}+\frac{\dot{q}\delta}{\rho_{la}C_p}. \tag{12}$$

Integrating equation (8) between a location y to δ and using the boundary condition (10b) on pressure P_m, we obtain

$$-P_m(y,x) = g\rho_{la}[\alpha(\delta-y)+\beta\int_y^\delta (T-T_a)\,dy]. \tag{13}$$

Let us assume the following profiles for velocity and temperature

$$\frac{u}{U} = \eta(1-\eta)^2, \quad \theta = \frac{T-T_a}{T_w-T_a} = (1-\eta)^2. \tag{14a,b}$$

These profiles clearly satisfy the boundary conditions given by equation (10). The substitution of equation (14b) into equation (13) gives

$$-P_m(\eta,x) = g\rho_{la}\delta[\alpha(1-\eta)+\beta\Delta T_w\left(\frac{1}{3}-\eta+\eta^2-\frac{\eta^3}{3}\right)] \tag{15}$$

$$-\frac{\partial P_m}{\partial x} = g\rho_{la}\left[\alpha+\beta\Delta T_w\left(\frac{1}{3}-\eta^2+\frac{2}{3}\eta^3\right)\right]\frac{d\delta}{dx}. \tag{16}$$

The use of equations (14) and (16) in equations (11) and (12) gives

$$\frac{1}{105}\frac{d}{dx}(\delta U^2) = \frac{1}{6}g\delta(\beta\Delta T_w+6\alpha)\frac{d\delta}{dx}-\frac{\nu U}{\delta} \tag{17}$$

$$\frac{1}{30}\frac{d(\delta U)}{dx} = \frac{2\lambda}{\delta}+\frac{\dot{q}\delta}{\rho_{la}C_p\Delta T_w}. \tag{18}$$

Nondimensionalizing the above equations by introducing the following nondimensional variables $\delta^* = \delta/\delta_s$, $x^* = x/L$, $U^* = U/U_s$, we obtain

$$\frac{1}{105}\frac{d(\delta^*U^{*2})}{dx^*} = \frac{1}{6}\frac{g\delta_s}{U_s^2}(\beta\Delta T_w+6\alpha)\times\left(\delta^*\frac{d\delta^*}{dx^*}\right)-\frac{L}{\delta_s}\frac{\nu}{U_s\delta_s}\left(\frac{U^*}{\delta^*}\right) \tag{19}$$

$$\frac{1}{30}\frac{d(\delta^*U^*)}{dx^*} = \left(\frac{L}{\delta_s}\right)\left(\frac{\nu}{U_s\delta_s}\right)\frac{2}{Pr}\frac{1}{\delta^*}+\frac{\dot{q}L\delta^*}{\rho_{la}C_p\Delta T_wU_s}. \tag{20}$$

If we choose the following scales

$$\delta_s = \left(\frac{\nu L}{U_s}\right)^{1/2} = \frac{L}{Gr_L^{1/5}}, \quad U_s = [g(\beta\Delta T_w+6\alpha)\sqrt{(\nu L)}]^{2/5} \tag{21a}$$

and the perturbation parameter as

$$\varepsilon = \frac{\dot{q}L}{\rho_{la}C_p\Delta T_w[g(\beta\Delta T_w+6\alpha)\sqrt{(\nu L)}]^{2/5}} \tag{21b}$$

then in the limit as $\varepsilon \to 0$ we have

$$\frac{1}{105}\frac{dU^{*2}\delta^*}{dx^*} = O(1), \quad \frac{\delta^*}{6}\frac{d\delta^*}{dx^*} = O(1), \quad \frac{U^*}{\delta^*} = O(1). \tag{21c}$$

With the choice of scales given by equation (21), equations (19) and (20) become

$$\frac{1}{105}\frac{d(\delta^*U^{*2})}{dx^*} = \frac{1}{6}\delta^*\frac{d\delta^*}{dx^*}-\frac{U^*}{\delta^*} \tag{22}$$

$$\frac{1}{30}\frac{d(\delta^*U^*)}{dx^*} = \frac{2}{Pr}\frac{1}{\delta^*}+\varepsilon\delta^*. \tag{23}$$

The effect of internal heat generation in the boundary layer will be included through the perturbation parameter, ε.

Seeking solution of equations (22) and (23) in the form

$$U^* = \sum_{k=0}^{\infty}\varepsilon^k U_k, \quad \delta^* = \sum_{k=0}^{\infty}\varepsilon^k\delta_k. \tag{24}$$

Substituting the above expansion into equations (22) and (23) and equating terms of like coefficients up to ε, we obtain

$$\varepsilon^0: \frac{1}{105}\frac{d(U_0^2\delta_0)}{dx^*} = \frac{1}{6}\delta_0\frac{d\delta_0}{dx^*}-\frac{U_0}{\delta_0} \tag{25a}$$

$$\frac{1}{30}\frac{d(U_0\delta_0)}{dx^*} = \frac{2}{Pr}\frac{1}{\delta_0} \tag{25b}$$

$$\varepsilon^1: \frac{1}{105}\frac{d}{dx^*}(U_0^2\delta_1+2U_0U_1\delta_0)$$

$$=\frac{1}{6}\left(\delta_1\frac{d\delta_0}{dx^*}+\delta_0\frac{d\delta_1}{dx^*}\right)-\left(\frac{U_1}{\delta_0}-\frac{U_0\delta_1}{\delta_0^2}\right) \quad (26a)$$

$$\frac{1}{30}\frac{d}{dx^*}(U_0\delta_1+U_1\delta_0)=-\frac{2}{Pr}\frac{\delta_1}{\delta_0^2}+\delta_0. \quad (26b)$$

We assume a solution of the form

$$U_k = A_k x^{*m} x^{*2kn} \quad \text{for} \quad k=0,1,2,\ldots \quad (27a)$$

$$\delta_k = B_k x^{*n} x^{*2kn} \quad \text{for} \quad k=0,1,2,\ldots \quad (27b)$$

The substitution of equation (27) in equation (25) yields

$$m=1/5, \quad n=2/5,$$

$$A_0=\frac{Pr^{-1/5}}{\left[\frac{3}{200}\left(\frac{16}{21}+Pr\right)\right]^{2/5}} \quad (28a)$$

$$B_0=\left[1500\left(\frac{16}{21}+Pr\right)\right]^{1/5}Pr^{-2/5}. \quad (28b)$$

The substitution of equation (27) in equation (26) gives

$$B_1=\frac{\frac{150}{7}\left(\frac{16}{35}A_0B_0+\frac{15}{B_0}\right)}{30\frac{A_0}{B_0^2}+4B_0+\frac{8}{35}A_0^2+\frac{32}{35}\frac{A_0}{Pr\,B_0^2}+\frac{30}{Pr\,B_0^4}} \quad (29a)$$

$$A_1=\frac{150}{7}-\frac{A_0}{B_0}+\frac{2}{Pr\,B_0^3}B_1. \quad (29b)$$

Now, using equations (27) and the values of m and n given by equation (28a), in equation (24), we obtain the following two-term expansions

$$U^*=A_0x^{*1/5}+\varepsilon A_1x^* \quad (30a)$$

$$\delta^*=B_0x^{*2/5}+\varepsilon B_1x^{*6/5}. \quad (30b)$$

Heat transfer coefficient

From the definition of Nusselt number and equations (14), (21), (28), and (30), we obtain

$$Nu_x=\frac{q_wx}{K(T_w-T_a)}=\frac{2x}{\delta}=\frac{2B_0^*\,Ra_x^{1/5}}{1+\varepsilon_mB_1^*\,Ra_x^{4/5}} \quad (31a)$$

where

$$B_0^*=\frac{1}{B_0\,Pr^{1/5}}=\frac{Pr^{1/5}}{\left[1500\left(\frac{16}{21}+Pr\right)\right]^{1/5}}, \quad (31b)$$

$$B_1^*=\frac{B_1}{B_0\,Pr^{4/15}}=\frac{B_1\,Pr^{2/15}}{\left[1500\left(\frac{16}{21}+Pr\right)\right]^{1/5}}$$

$$\varepsilon_m=\frac{\nu^{1/3}}{[(\beta\Delta T_w+6\alpha)g]^{2/3}}\left(\frac{\dot q}{\rho_{la}C_p\Delta T_w}\right) \quad (31c)$$

$$Ra_x=Pr\,Gr_x, \quad Gr_x=(\beta\Delta T_w+6\alpha)gx^3/\nu^2. \quad (31d)$$

From the definition of ε_m and equation (21b), it is clear that $\varepsilon_m=\varepsilon$ if the length scale L is chosen as

$$L=\frac{\nu^{2/3}}{[(\beta\Delta T_w+6\alpha)g]^{1/3}}. \quad (32a)$$

With the above choice of the length scale, U_s and δ_s as given by equation (21a) become

$$U_s=[\nu(\Delta T_w+6\alpha)g]^{1/3}, \quad \delta_s=\frac{\nu^{2/3}}{[(\beta\Delta T_w+6\alpha)g]^{1/3}}. \quad (32b)$$

It is clear that with the choice of scales as given by equations (32), the requirement imposed by equation (21c) on the order of various terms is still satisfied. With these scales, it is evident that for the perturbation scheme to work, we must have

$$\varepsilon=\varepsilon_m=\frac{\nu^{1/3}}{[(\beta\Delta T_w+6\alpha)g]^{2/3}}\left(\frac{\dot q}{\rho_{la}C_p\Delta T_w}\right)\ll 1. \quad (33)$$

The typical values of ε for application to transition phase of a hypothetical core disruptive accident with $\alpha=0.1$, $\dot q=175.86\times10^6$ W m^{-3}, $\Delta T_w=24$ K, $\varepsilon\simeq 3\times10^{-3}$. This value of ε corresponds to boiling pool consisting of a mixture of stainless steel and molten fuel with stainless steel boiling. In other applications the values of ε are expected to be even smaller. For example, in experiments by Gabor *et al.* [3], the values of ε are of the order of 10^{-4}. Therefore, in applications that we are considering, equation (33) is readily satisfied. Consequently in the limit as $\varepsilon\to 0$, i.e. with negligible effect of internal heat generation, equation (31a) becomes

$$Nu_x=2B_0^*\,Ra_x^{1/5}=\frac{2Pr^{1/5}}{\left[1500\left(\frac{16}{21}+Pr\right)\right]^{1/5}}Ra_x^{1/5}. \quad (34)$$

The above expression agrees within error of about 5% with the exact expression given as

$$Nu_x=0.394Pr^{1/20}\,Ra_x^{1/5}. \quad (35)$$

This expression is obtained by Pera and Gebhart [7] for the case of single-phase heat transfer driven by temperature gradient alone. However, in comparison between these two expressions, it is assumed that the Grashof number to be used in expression (35) is the two-phase Grashof number defined by equation (31d). From expressions (28) it is clear that the two constants A_0 and B_0 are positive numbers, and hence B_1 given by expression (29a) is also a positive number. This in turn implies that the boundary layer thickness given by equation (30b) will increase with internal heat generation and the heat transfer coefficient given by equation (31a) will decrease as the internal heat generation rate increases. This effect of internal heat generation is quite opposite to the effect on heat transfer from vertical or inclined walls of the boiling pool. As in the latter case, the internal heat generation tends to increase the heat transfer coefficient [6]. Another distinction between the two cases is that the Grashof

number for the case of heat transfer from vertical walls is based on $Gr_x = (\beta\Delta T_w + 3\alpha)gx^3/\nu^2$ instead of its definition as given by equation (31d) for the case of the horizontal base of the pool. Furthermore, the Nusselt number varies as one-fourth of the power of the Rayleigh number for the case of vertical walls as against one-fifth power in the present case.

The effect of internal heat generation in the case of the turbulent boundary layers to be discussed in the following section is expected to be small in view of the fact that the boundary layer is considerably thicker than that for the laminar flow and the temperature profile is significantly steeper near the wall than for the laminar flow. Consequently, the perturbation caused by internal heat generation in the boundary layer thickness and on the temperature profile for turbulent flow will be relatively less significant than for the laminar flow. In view of these comments, we will not consider the effect of internal heat generation for the case of turbulent flow.

TWO-LAYER MODEL OF TURBULENT LAYERS

The integral method utilized for laminar flow proved to be very successful (the error in the expression for the Nusselt number is less than 6% from the exact analysis). However, similar analysis for turbulent flow cannot be performed as velocity and temperature profiles cannot be prescribed with any degree of satisfaction, since the behavior in the inner part of the boundary layer is definitely different from that in the outer part. Consequently, these integral approaches have to be augmented by experimental data near the wall. Even then a reasonable accuracy is not assured. To circumvent these difficulties we resort to an alternative approach based on a two-layer model of the turbulent boundary layer. This approach had a very measurable success in the case of heat transfer from the vertical wall of the boiling pools [6]. This approach has also been used very successfully by George and Capp [8] for the single-phase natural convection flows along the vertical wall and by Long [9] for the case of single-phase natural convection flow in horizontal layers.

In the analysis to be presented we will extend the use of the two-layer model to the combined temperature and two-phase buoyancy driven turbulent boundary layer existing next to the base of the boiling pools. Analogous to turbulent boundary flows in forced flow, George and Capp [8] have shown that the fully developed turbulent boundary layer in the temperature driven natural convection also consists of two regions: a thin diffusion-controlled inner region and an outer region constituting most of the boundary layer in which viscous and conduction terms are negligible. They further identify that the inner region is a constant heat flux layer made up of two major subdivisions: an inner subregion consisting of a conductive and viscous sublayer existing right next to the wall and an outer subregion existing at the outer part of the constant heat flux layer which is referred to as the buoyant sublayer. An asymptotic matching in the buoyant sublayer between the inner and outer layers yields velocity and temperature profiles. These universal similarity laws, in turn, yield asymptotic heat transfer and friction laws.

As already mentioned, the scaling laws for the laminar flow as given by equation (32) are different from those used for laminar flow along the vertical walls. One may expect similar differences for the case of turbulent flows. The scaling laws obtained by both George and Capp [8] and by Long [9] are based on dimensional analysis, whereas in the present analysis we will obtain these scaling laws formally from the governing equations by assuming separate similarity solutions for the inner and outer layers. This approach is similar to one used previously for the vertical walls of the pool [6].

Scaling of buoyancy term

The integral equations (19) and (20) or equations (22) and (23), describing the laminar flow, clearly show that buoyancy $\rho_{1a}(\beta\Delta T + \alpha)g$ term occurring in equation (8) should be scaled by $\rho_{1a}(\beta\Delta T_w + 6\alpha)g$ to yield the velocity scale given by equation (32). In the turbulent boundary layer driven by temperature difference alone, the inner and outer scales for the buoyancy terms are clearly determined by the choices for temperature scales for the two layers. However, for the case of two-phase driven flows, the buoyancy contribution $\alpha g\rho_{1a}$ is generated outside the boundary layer and remains invariant both in the inner and outer layers. Hence, for this contribution to survive in the momentum equations governing the inner and outer layers, we must use the same scale for the two layers. In the inner layer, however, where most of the temperature drop occurs (this follows from the analogy with the forced convection), it is clear that $\Delta T = O(\Delta T_w)$, and hence $(\beta\Delta T + \alpha) = O(\beta\Delta T_w + 6\alpha)$, where a factor of six for α is preserved by analogy with the laminar case with an aim to show an equivalence between the two-phase driven flows and those driven by thermal expansion alone. As long as the two-phase buoyancy contribution dominates, it is appropriate to use the same scale, namely, $(\beta\Delta T_w + 6\alpha)$ both in the inner and outer layers.

The inner layer. Let us assume a similarity solution of the form

$$U = U_I f'(\xi, Pr), \quad T - T_w = \Delta T_I \theta(\xi, Pr) \tag{36a}$$

$$-\overline{u'v'} = u_s^2 G_I(\xi, Pr), \quad -\overline{v'T'} = \Phi_I \phi_I(\xi, Pr) \tag{36b}$$

$$P_m = \rho_{1a} U_I^2 P_I^*(\xi, Pr),$$

$$\beta\Delta T + \alpha = (\beta\Delta T_w + 6\alpha)H_I(\xi, Pr). \tag{36c}$$

Substituting equations (36) in equations (9), (8), and (4) and using equation (1), we obtain

$$\frac{\Lambda}{U_I}\frac{dU_I}{dx}(f'^2 - ff'') - \frac{d\Lambda}{dx}ff'' = -\Lambda\frac{\partial P_I^*}{\partial x} - \frac{\Lambda P_I^*}{U_I}\frac{dU_I}{dx} + \frac{\nu f'''}{\Lambda U_I} + \frac{U_s^2}{U_I}G_I' \tag{37a}$$

$$\frac{\partial P_I^*}{\partial \xi} = P_I^{*\prime} = \frac{\Lambda g}{U_I^2}(\beta \Delta T_w + 6\alpha) H_I \tag{37b}$$

$$\frac{\Lambda}{\Delta T_I}\frac{d\Delta T_I}{dx} f'\theta - \frac{d\Lambda}{dx} + \frac{\Lambda}{U_I}\frac{dU_I}{dx} f\theta' = \frac{\lambda}{U_I \Lambda}\theta' + \frac{\Phi_I}{U_I \Delta T_I}\phi_I'. \tag{37c}$$

For the horizontal base as can be seen from equations (37a) and (37b), pressure P_m gives the driving mechanism for the fluid flow. Because of the buoyancy generated by two-phase volume boiling, the bulk fluid rises up and sets up a negative pressure gradient along the base. This in turn causes the boundary layer to flow over the base plate. Consequently, in the inner layer not only molecular and turbulent diffusion terms dominate but also the contribution of the pressure gradient must be retained in the inner layer. These considerations lead us to the following choice for the various scales

$$\Lambda = \lambda / U_I, \quad \Phi_I = \Delta T_I U_I, \quad u_s = U_I \tag{38a}$$

$$U_I = [(\beta \Delta T_w + 6\alpha) g \Lambda]^{1/2} = [(\beta \Delta T_w + 6\alpha) g \lambda]^{1/3} \tag{38b}$$

$$\Lambda = \lambda^{2/3} / [(\beta \Delta T_w + 6\alpha) g]^{1/3}. \tag{38c}$$

From equation (38a), we can write

$$\Delta T_I = \Lambda \Phi_I / \lambda = \Delta T_w \tag{38d}$$

where we have used the fact that $\Delta T_I = \Delta T_w$.

In the above choice for length scale Λ, it is implicit that $Pr = O(1)$. From equations (38) it is clear that U_I, Λ, and Φ_I are not functions of x, hence equations (37) simplify to

$$0 = -\Lambda \frac{\partial P_I^*}{\partial x} + Pr\, f''' + G_I' \tag{39a}$$

$$P_I^{*\prime} = H_I \tag{39b}$$

$$0 = \theta'' + \phi_I'. \tag{39c}$$

The integration of equation (39c) together with equation (38d) gives

$$\theta' + \phi_I = -\frac{q_w}{\rho_{la} C_p \Phi_I}. \tag{40}$$

From the above equation it is clear the scale Φ_I must be chosen as

$$\Phi_I = \frac{q_w}{\rho_{la} C_p}. \tag{41}$$

It is also clear from equation (40) that the inner layer is a constant flux layer. However, in the outer layer heat flux must vanish at the outer edge and must be equal to q_w at its inner edge. It then follows that the scale Φ_0 for the heat flux in the outer layer is also given by equation (41), that is

$$\Phi_0 = \frac{q_w}{\rho_{la} C_p}. \tag{42}$$

The outer layer. For the outer layer, by analogy to the forced convection case, we assume the similarity solution to be of the form

$$\frac{u - U_m}{u_0} = F'(\eta), \quad \frac{T - T_a}{\Delta T_0} = \Psi(\eta) \tag{43a}$$

$$-\overline{u'v'} = u_\tau^2 G_0(\eta), \quad -\overline{v'T'} = \Phi_0 \phi_0(\eta) \tag{43b}$$

$$\beta \Delta T + \alpha = (\beta \Delta T_w + 6\alpha) H_0(\eta), \quad P_m = \rho_{la} U_m^2 P_0^*(\eta). \tag{43c}$$

The use of equations (43) in equations (1), (9), (8) and (4) gives

$$\frac{\delta}{U_m}\frac{dU_0}{dx}(F'^2 - FF'') + \frac{\delta}{U_m}\frac{dU_m}{dx}(F' - \eta F'') + \frac{\delta}{U_0}\frac{dU_0}{dx}F' - \frac{d\delta}{dx}\eta F'' - \frac{u_0}{U_m}\frac{d\delta}{dx}FF'' + \frac{\delta}{u_0}\frac{dU_m}{dx} = -\frac{2\delta}{u_0}\frac{dU_m}{dx}P_0^* - \frac{\delta U_m}{u_0}\frac{\partial P_0^*}{\partial x} + \frac{\nu}{\delta U_m}F''' + \frac{u_\tau^2}{u_0 U_m}G_0' \tag{44a}$$

$$P_0^{*\prime} = \frac{\delta(\beta \Delta T_w + 6\alpha) g}{U_m^2} H_0(\eta) \tag{44b}$$

$$\frac{d\delta}{dx}\left[\frac{\delta}{\Delta T_0}\frac{d\Delta T_0}{d\delta}\left(F' + \frac{U_m}{u_0}\right)\Psi - \frac{U_m}{u_0}\eta\Psi' - \frac{\delta}{u_0}\frac{du_0}{d\delta}F\Psi' - F\Psi' - \frac{\delta}{u_0}\frac{dU_m}{d\delta}\eta\Psi'\right] = \frac{1}{Pr}\frac{\nu}{\delta u_0}\Psi'' + \frac{\Phi_0}{u_0 \Delta T_0}\phi_0'. \tag{44c}$$

Since by assumption the outer layer is dominated by mean convection, turbulent diffusion, and buoyancy terms, equations (44) will have similarity solution provided the following conditions are satisfied

$$u_0 = U_m \tag{45a}$$

$$\frac{d\delta}{dx} = C_1 \tag{45b}$$

$$\frac{\delta}{u_0}\frac{du_0}{dx} = C_2 \tag{45c}$$

$$\frac{\delta}{\Delta T_0}\frac{d\Delta T_0}{dx} = C_3 \tag{45d}$$

$$u_\tau = u_0 \tag{45e}$$

$$u_0 = U_m = \sqrt{(g(\beta \Delta T_w + 6\alpha))\delta} \tag{45f}$$

$$\Phi_0 = u_0 \Delta T_0 = q_w / \rho_{la} C_p \tag{45g}$$

where in equation (45g), we have substituted for Φ_0 from equation (42). Condition (45b) implies that $\delta \sim x$. In view of equation (45b), equations (45c) and (45d) can be written as

$$\frac{\delta}{u_0}\frac{du_0}{d\delta} = b, \quad \frac{\delta}{\Delta T_0}\frac{d\Delta T_0}{d\delta} = d \tag{46}$$

where b and d are constants. Equations (46) yield

$$u_0 = a\delta^b, \quad \Delta T_0 = C\delta^d \tag{47}$$

where a and c are integration constants. The combination of equations (45f) and (45g) give

$$\Delta T_0 = \frac{\Phi_0}{u_0} = \frac{\Phi_0}{[(\beta\Delta T_w + 6\alpha)g\delta]^{1/2}}$$

$$= \frac{q_w}{\{\rho_{la} C_p[(\beta\Delta T_w + 6\alpha)g\delta]^{1/2}\}}. \tag{48}$$

The comparison of equations (47) with equations (45f) and (48) yields

$$a = [g(\beta\Delta T_w + 6\alpha)]^{1/2}, \quad b = \frac{1}{2}, \quad d = -\frac{1}{2} \tag{49a}$$

$$c = \frac{\Phi_0}{[(\beta\Delta T_w + 6\alpha)g]^{1/2}}. \tag{49b}$$

Thus, the choice of scales given by equations (45f), (45g), and (48) together with the condition (45b) ensures the existence of similarity solution (43). Equation (44b) upon integration between the limits η to δ together with use of boundary condition (10b) gives

$$-P_0^*(\eta) = \int_\eta^\delta H_0(\eta)\, d\eta \tag{50a}$$

and

$$-\frac{\partial P_0^*}{\partial x} = \frac{2}{\delta}\frac{d\delta}{dx} H_0(\eta) - \frac{1}{\delta}\frac{d\delta}{dx} P_0^*. \tag{50b}$$

The use of equations (45), (46), and (49a) in equations (44a) and (44c) and then taking the limit $\delta u_0/\nu \to \infty$, yields

$$\frac{1}{2}\frac{d\delta}{dx}[F'^2 + 2F' - 3FF'' - 3\eta F'' + 1 + 4(P_0^*(\eta) - H_0(\eta))] = G_0'(\eta) \tag{51a}$$

$$-\frac{1}{2}\frac{d\delta}{dx}[(1-F')\Psi + 3\eta\Psi' + 3F\Psi'] = \phi_0'. \tag{51b}$$

For use in the subsequent analysis, it is also of interest to obtain the ratios of the inner to outer scales for velocity and temperature. From equations (38), (41), (45), and (48), we get

$$\frac{U_I}{u_0} = \left(\frac{\Delta}{\delta}\right)^{1/2} \tag{52a}$$

$$\frac{\Delta T_I}{\Delta T_0} = \left(\frac{\delta}{\Lambda}\right)^{1/2}. \tag{52b}$$

ASYMPTOTIC MATCHING

The adoption of a two-layer model has greatly simplified the governing equations. However, in spite of these simplifications of equations (39) for the inner layer and equations (51) for the outer layer, still these equations cannot be solved due to lack of closure laws for turbulent diffusion terms. Because of strong coupling between momentum and energy equations, traditional formulations for eddy diffusivities for momentum and heat transfer based on forced convection flows cannot be extended to the case of natural convection flows. An alternative approach is feasible. Since turbulent boundary layers have all the characteristics of singular-perturbation problems [10–12], some specific results can be obtained by carrying out asymptotic matching between the inner and the outer layers. The asymptotic constraints imposed on the velocity and temperature profiles make *ad hoc* assumptions on the relation between the Reynolds stress and the velocity gradient and between the turbulent heat diffusion and the temperature gradient unnecessary.

In the proposed two-layer model, we seek the solution for the inner layer in the form given by equation (36a) and for the outer layer in the form given by equation (43a). However, as shown by Tennekes and Lumley [10], the existence of a matched layer or a region of overlap between the inner and the outerlayers is possible only if the limits $\xi = y/\Lambda \to \infty$ and $\eta = y/\delta \to 0$ can be taken simultaneously. This, however, is possible since as Ra_δ or $Gr_\delta \to \infty$

$$\frac{\delta}{\Lambda} = \left(\frac{\nu}{\lambda}\right)^{2/3}[\beta\Delta T_w + 6\alpha)g\delta^3/\nu^2]^{1/3} = (Pr\ Ra_\delta)^{1/3} \to \infty. \tag{53}$$

Consequently, the principle of asymptotic matching when applied to temperature gradient yields

$$\lim_{\xi\to\infty}[\xi^{3/2}\theta'] = \lim_{\eta\to 0}[\eta^{3/2}\Psi'] = -\frac{\kappa}{2}. \tag{54}$$

The integration of this equation gives the temperature profiles as

$$\frac{T - T_w}{\Delta T_I} = \kappa\xi^{-1/2} + A(Pr) \tag{55a}$$

$$\frac{T - T_a}{\Delta T_0} = \kappa\eta^{-1/2} + B. \tag{55b}$$

Requiring now that these profiles themselves match at a given point in the overlap region, gives us

$$\frac{T_w - T_a}{\Delta T_I} = C'^{-1} = B\left(\frac{\Lambda}{\delta}\right)^{1/2} - A(Pr). \tag{56}$$

In obtaining the above relations, we have made use of equation (52b).

From equation (56) it is clear that

$$C'^{-1} \to -A(Pr) \quad \text{as} \quad \Lambda/\delta \to 0 \quad \text{or as} \quad Ra_\delta \to \infty \tag{57}$$

which shows that C' is a function of the Prandtl number. From equations (56), (38d), 38c), and (41), we obtain

$$C' = \frac{\Delta T_I}{T_w - T_\infty} = \frac{q_w L}{(T_w - T_a)K}\left\{\frac{(\lambda/\nu)^{2/3}}{[(\beta\Delta T_w + 6\alpha)gL^3/\nu^2]^{1/3}}\right\} \tag{58}$$

which yields

$$Nu = C'\ Pr^{-1/3}\ Ra^{1/3} = C(Pr)Ra^{1/3} \qquad (59)$$

where $C = Pr^{-1/3}\ C'$. From asymptotic relation (57), it is clear that C is function of the Prandtl number only.

The only single-phase reliable correlation with which above correlation can be compared with is due to Long [9] for the case of turbulent thermal convection in horizontal fluid layers. He obtained the following two correlations depending upon his assumed dependence of the temperature profile with the distance in the overlap region

$$Nu = \begin{cases} \dfrac{0.04356Ra^{1/3}}{[1-1.402(Ra\ Nu)^{-1/12}]^{4/3}} & \text{for } s = 1/3 \\ \dfrac{0.04786Ra^{1/3}}{[1-2.544(Ra\ Nu)^{-1/8}]^{4/3}} & \text{for } s = 1/2 \end{cases} \qquad (60a,b)$$

where $s = 1/3$ denotes inverse cube root profile and $s = 1/2$ inverse square root profile. Long's latter choice for temperature profile is the same as we have arrived at in equation (55). These correlations clearly show that as $Ra \to \infty$, $Nu \propto Ra^{1/3}$, which is in agreement with expression (59).

The data to be used for determining constant C in equation (59) is due to Gabor *et al.* [3]. The Prandtl number was varied between 2.38 and 3.08. This variation, however, is not large enough to determine reliably the dependence of C on Prandtl number. Consequently, we will assume C to be a constant. Figure 2 shows data of Gabor *et al.* plotted as Nu vs Ra. These data constitute about 76 data points. Maintaining a slope of one-third on the log–log scale as predicted by expression (59), we show in Fig. 2 the following least square fit through this data

$$Nu = 0.0375Ra^{1/3}. \qquad (61)$$

On the average, the data does appear to show a slope of one-third and thus signifies a satisfactory agreement of the theory with the data. Also shown in this figure are the two Long's correlations given by equation (60). The Rayleigh number used in these correlations is based on two-phase flow as defined by equation (31d). Over the range of these Rayleigh numbers there does not appear to be any significant difference between these two correlations by Long. The agreement between these correlations and that given by equation (61) appears to be within the scatter of data and improves as Rayleigh number increases. In fact, correlation (60a) differs by about 14% from the present correlation (61) as $Ra \to \infty$ which is well within the scatter of the data used here.

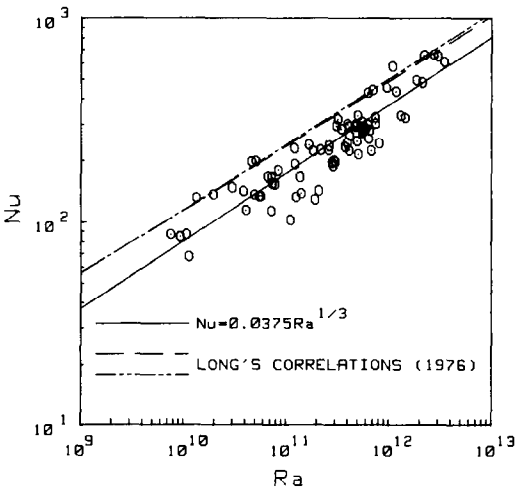

FIG. 2. Correlation of downward heat transfer coefficient data of Gabor *et al.* [3] and comparison with Long's correlations [9]. (– – –, inverse cube root temperature profile; – · · –, inverse square root temperature profile).

CONCLUSION

A comparison of the turbulent analysis with experimental data for the heat transfer coefficient from the horizontal base of the volume heated boiling pools and with existing empirical correlation by Long [9] obtained for temperature driven thermal convection in horizontal layers confirms the validity of the proposed heat transfer model, that is, heat transfer to the base of the boiling pool takes place through a single-phase turbulent boundary layer driven along the base by the buoyancy forces of the two-phase void distribution in the bulk of the pool. The analysis for the laminar case shows that the combined (or opposing) two-phase and temperature driven natural convection along the base of pool is characterized by Grashof number, $Gr = (\beta\Delta T_w + 6\alpha)gL^3/\nu^2$. With this definition of Gr, both for laminar and turbulent flows, the analysis shows that an equivalence exists between the heat transfer laws for the combined two-phase and thermal expansion driven natural convection and the laws for temperature driven natural convection alone.

REFERENCES

1. A. Markowitz and A. E. Bergles, Operational limits of a submerged condenser, *Prog. Heat Mass Transfer* **6**, 701–716 (1972).
2. R. P. Stein, J. C. Hesson and W. H. Gunther, Studies of heat removal from heat generating boiling pools, in *Proc. Fast Reactor Safety Meeting*, Beverly Hills, California, CONF-740401-P2, pp. 865–880 (1974).
3. J. D. Gabor, L. Baker, Jr., J. C. Cassulo and G. A. Mansoori, Heat transfer from heat generating boiling pools, *A.I.Ch.E. Symp. Ser.* **73**, 78–85 (1976).
4. I. K. Paik, S. I. Abdel-Khalik, R. G. Cepress and H. S. Kim, On the heat transfer characteristics of molten core debris pools growing in concrete, *Nucl. Eng. Des.* **64**, 149–150 (1981).
5. G. A. Greene and C. E. Schwarz, An approximate model for calculating overall heat transfer between overlying immiscible liquid layers with bubble-induced liquid entrainment, *Proc. 5th Post Accident Heat Removal Information Exchange Meeting*, Nuclear Research Center Karlsruhe, Karlsruhe, 28–30 July, pp. 251–257 (1982).
6. T. C. Chawla and S. H. Chan, Heat transfer from vertical/inclined boundaries of heat-generating boiling pools, *J. Heat Transfer* **104**, 465–473 (1982).
7. L. Pera and B. Gebhart, Natural convection boundary layer flow over horizontal and slightly inclined surfaces, *Int. J. Heat Mass Transfer* **16**, 1131–1146 (1973).
8. W. K. George, Jr. and S. P. Capp, A theory for natural

convection turbulent boundary layers next to heated vertical surfaces, *Int. J. Heat Mass Transfer* **22**, 813–826 (1979).
9. R. R. Long, Relation between Nusselt number and Rayleigh number in turbulent thermal convection, *J. Fluid Mech.* **73**, 445–451 (1976).
10. H. Tennekes and J. L. Lumley, *A First Course in Turbulence*. MIT Press, Cambridge, Massachusetts (1972).
11. H. Tennekes, Outline of a second-order theory of turbulent pipe flow, *AIAA J.* **6**, 1735–1740 (1968).
12. T. C. Chawla and H. Tennekes, Turbulent boundary layers with negligible wall stress: a singular-perturbation theory, *Int. J. Engng Sci.* **11**, 45–65 (1973).

TRANSFERT THERMIQUE PAR EBULLITION DANS DES RESERVOIRS

Résumé—On propose un modèle pour le transfert thermique à partir de la base horizontale d'un volume chauffé par ébullition en réservoir. A cause de la différence de densité entre la masse fluide et le fluide proche de la base, le fluide diphasique plus léger cause le mouvement de la masse dans la direction ascendante et provoque un gradient négatif de pression le long de la base du réservoir. Cette pression négative provoque le retour du liquide monophasique froid dans la couche limite de la base. L'analyse pour le cas laminaire fournit la définition d'un nombre de Grashof équivalent pour la convection naturelle le long de la base plane. La couche limite turbulente est analysée en supposant un modèle à deux couches dans lequel la couche interne est caractérisée par des termes visqueux et de conduction et la couche externe par des termes de convection moyenne. L'analyse de similitude des équations fournit des profils universels de température et de vitesse et les lois pour les deux couches. Une atteinte asymptotique du profil de température dans la région de recouvrement conduit à une loi de transfert thermique qui représente bien les données expérimentales disponibles sur l'ébullition en réservoir.

ABWÄRTS GERICHTETER WÄRMETRANSPORT IN WÄRMEERZEUGENDEN SIEDEBEHÄLTERN

Zusammenfassung—Es wird ein Modell für den Wärmeübergeng an der horizontalen Bodenplatte eines volumenbeheizten Siedebehälters vorgeschlagen. Aufgrund der Dichteunterschiede zwischen dem Kernfluid und dem bodennahen Fluid, die durch das 'Volumensieden' hervorgerufen werden, verursacht das leichtere zweiphasige Fluid aufwärtsgerichtete Strömungen des Kernfluids sowie einen negativen Druckgradienten längs des Behälterbodens. Dieser negative Druckgradient bewirkt ein Nachströmen unterkühlter einphasiger Flüssigkeit in die Grenzschicht der Bodenplatte. Die Untersuchung des laminaren Falls erbrachte die Definition einer äquivalenten Grashof-Zahl für die gleichsinnig (oder gegensinnig) gerichtete natürliche Konvektion entlang der Bodenplatte aufgrund der Temperaturunterschiede und der zweiphasigen Strömung. Die turbulente Grenzschicht wurde mit Hilfe der Annahme eines Zweischichtenmodells untersucht, bei dem die innere Schicht durch Viskositäts- und Wärmeleitungsterme charakterisiert ist und die äußere Schicht durch mittlere Konvektionsterme. Die Ähnlichkeitsbetrachtungen der maßgeblichen Gleichungen liefern universelle Temperatur- und Geschwindigkeitsprofile sowie die Maßstabsfaktoren der inneren und äußeren Schicht. Ein asymptotisches Anpassen der Temperaturprofile in der Überschneidungszone führt zu einer Wärmeübergangsbeziehung, welche die verfügbaren experimentellen Daten volumenbeheizter Siedebehälter zufriedenstellend korreliert.

ТЕПЛОПЕРЕНОС В ТЕПЛОВЫДЕЛЯЮЩИХ БОЛЬШИХ ОБЪЕМАХ ЖИДКОСТИ ПРИ КИПЕНИИ

Аннотация—Предложена модель теплопереноса от горизонтального основания большого объема нагреваемой жидкости. Из-за вызванной кипением разности плотностей между основной массой жидкости и ее частью у основания более легкая двухфазная жидкость приводит в движение основную массу жидкости по направлению вверх, в результате чего возникает отрицательный градиент давления вдоль нижней поверхности контейнера. В свою очередь это приводит в движение массу переохлажденной однофазной жидкости в пограничном слое вдоль основания контейнера. Анализ ламинарного случая позволяет о определить эквивалентное число Грасгофа для смешанной конвекции для двухфазных потоков. Турбулентный пограничный слой анализируется в предположении двухслойной модели, в которой внутренний слой характеризуется вязкими и кондуктивными членами, а внешний слой – средними конвективными членами. Анализ основных уравнений с помощью теории подобия позволяет получить универсальные профили температуры и скорости и критерии подобия для внутренних и внешних слоев. С помощью асимптотического сращивания температурного профиля в области перекрытия получен закон теплопереноса, который удовлетворительно обобщает имеющиеся экспериментальные данные по кипению в большом объеме жидкости.